BMC Cardiovascular Disorders

RESEARCH

Open Access

RING finger protein 5 protects against acute myocardial infarction by inhibiting ASK1

Hong Wan[1†], Jianqing Zhang[2†], Zhen Liu[3], Bizhen Dong[4], Zhangqian Tao[3], Guanglin Wang[5*] and Chihua Wang[6*]

Abstract

Background Myocardial infarction (MI) is a major disease with high morbidity and mortality worldwide. However, existing treatments are far from satisfactory, making the exploration of potent molecular targets more imperative. The E3 ubiquitin ligase RING finger protein 5 (RNF5) has been previously reported to be involved in several diseases by regulating ubiquitination-mediated protein degradation. Nevertheless, few reports have focused on its function in cardiovascular diseases, including MI.

Methods In this study, we established RNF5 knockout mice through precise CRISPR-mediated genome editing and utilized left anterior descending coronary artery ligation in 9-11-week-old male C57BL/6 mice. Subsequently, serum biochemical analysis and histopathological examination of heart tissues were performed. Furthermore, we engineered adenoviruses for modulating RNF5 expression and subjected neonatal rat cardiomyocytes to oxygen-glucose deprivation (OGD) to mimic ischemic conditions, demonstrating the impact of RNF5 manipulation on cellular viability. Gene and protein expression analysis provided insights into the molecular mechanisms. Statistical methods were rigorously employed to assess the significance of experimental findings.

Results We found RNF5 was downregulated in infarcted heart tissue of mice and NRCMs subjected to OGD treatment. RNF5 knockout in mice resulted in exacerbated heart dysfunction, more severe inflammatory responses, and increased apoptosis after MI surgery. In vitro, RNF5 knockdown exacerbated the OGD-induced decline in cell activity, increased apoptosis, while RNF5 overexpression had the opposite effect. Mechanistically, it was proven that the kinase cascade initiated by apoptosis signal-regulating kinase 1 (ASK1) activation was closely regulated by RNF5 and mediated RNF5's protective function during MI.

Conclusions We demonstrated the protective effect of RNF5 on myocardial infarction and its function was dependent on inhibiting the activation of ASK1, which adds a new regulatory component to the myocardial infarction associated network and promises to enable new therapeutic strategy.

Keywords RNF5, Myocardial infarction , Inflammation, Apoptosis, ASK1

†Hong Wan and Jianqing Zhang contributed equally to this work.

*Correspondence:
Guanglin Wang
2285532569@qq.com
Chihua Wang
wangchihua@hgyy.org.cn
[1]General practice medicine, Huanggang Central Hospital of Yangtze University, Huanggang, China
[2]Department of central laboratory, Renmin hospital of Wuhan university, Wuhan, China
[3]Department of Cardiology, Renmin hospital of Wuhan university, Wuhan, China
[4]Huanggang Institute of Translational Medicine, Huanggang, China
[5]Department of Cardiology, Huanggang Central Hospital of Yangtze University, Huanggang, China
[6]Huanggang Disease Control Center, Huanggang, China

Introduction

Myocardial infarction (MI), pathologically defined as myocardial cell death due to prolonged ischemia, stands as one of the major causes of mortality worldwide [1–3]. The resultant ischemic injury from MI triggers an extensive inflammatory response, mobilizing diverse populations of innate and adaptive immune cells during the early stages of MI, and accompanied by increased secretion of inflammatory cytokines [4, 5]. Furthermore, post-MI, the myocardial tissue in the infarct and peri-infarct areas undergoes apoptosis due to ischemia, hypoxia, and extensive inflammatory reactions, thereby serving as a critical determinant of the severity of post-MI cardiac failure [6, 7]. Despite substantial efforts to understand the molecular basis of this pathological process, available therapeutic development remains far from satisfactory. This highlights the pressing need to identify potent molecular targets for regulating MI.

RING finger protein 5 (RNF5), also known as RMA1, is an endoplasmic reticulum (ER)-localized 18-kDa RING finger E3 ligase with a RING finger motif and a C-terminal membrane-anchoring domain [8, 9]. RNF5 is primarily involved in endoplasmic reticulum-associated degradation (ERAD) to regulate protein stability through ubiquitination-mediated protein degradation. However, in some cases, it may affect protein–protein interactions through ubiquitination [10, 11]. Over the past two decades, extensive research has been conducted on RNF5's function in tumor progression, the innate immune response, and particularly in cystic fibrosis therapy development [12–14]. To date, RNF5 has been reported to play various roles in different cancers, exhibiting protumorigenic roles in some, antitumorigenic roles in others, and dual roles in breast cancer [12, 15–19]. Additionally, in the innate immune response, RNF5 has been implicated in post-infection responses to various viruses, including COVID-19, influenza A virus, and pseudorabies virus, through its regulation of the stability of key antiviral modulators, such as STING (stimulator of interferon gene) and MAVS (mitochondrial antiviral-signaling protein) [13, 20–22]. Notably, in cystic fibrosis (CF), RNF5 inhibition was found to promote significant F508del-CFTR (CF transmembrane conductance regulator) rescue, offering a promising strategy for the treatment of CF [14, 23, 24].

However, research on RNF5 in cardiovascular or related diseases remains limited. Existing studies have indicated that RNF5 attenuates pathological cardiac hypertrophy and that RNF5 deficiency exacerbates myocardial fibrosis and inflammation [25]. In nonalcoholic steatohepatitis (NASH), RNF5 overexpression has been shown to mitigate lipid accumulation and inflammation in hepatocytes, while hepatocyte-specific RNF5 knockout significantly worsened hepatic steatosis, the inflammatory response, and fibrosis in mice challenged with diet-induced NASH [26]. Moreover, decreased RNF5 expression was observed in H9C2 cells after oxygen-glucose deprivation/reperfusion (OGD/R) treatment, with RNF5 overexpression reversing the OGD/R-induced decrease in cell viability, apoptosis rate, and release of inflammatory factors [27]. However, this research was limited to the H9C2 cell line in vitro, and the function of RNF5 in MI has not yet been explored.

Therefore, we investigated RNF5's effects on MI and found that RNF5 expression levels were correlated with MI in vivo and in vitro. RNF5-knockout (KO) mice exhibited exacerbated heart dysfunction and more severe inflammatory response and apoptosis after MI surgery. Consistently, RNF5 knockdown exacerbated the cell apoptosis rate induced by OGD treatment in neonatal rat cardiac myocytes (NRCMs), while RNF5 overexpression alleviated it. Importantly, the kinase cascade initiated by apoptosis signal-regulating kinase 1 (ASK1) activation was found to be under the control of RNF5 and mediated the ameliorative effects of RNF5 on apoptosis in vitro. Our findings shed light on a new landscape of RNF5 in MI and hold promise for possible therapeutic development based on the RNF5-ASK1 axis.

Materials and methods

Experimental mice and acute myocardial infarction models

Using the CRISPR online design tool (http://chopchop.cbu.uib.no/) to predict target DNA regions boots sequence-guide RNA target site: GCCCCGCTCGCGAT TTGGCCCTTCGGG. RNF5-sgRNA expression vector was constructed using pUC57-sgRNA (51132, Addgene) as skeleton vector to construct RNF5 knockout (KO) mice. The in vitro transcripts of Cas9 expression vector pST1374-Cas9 (44758, Addgene) and sgRNA expression vector were purified, recovered, and configured into a mixed system (Cas9 mRNA: 10 ng/μL; sgRNA: 10 ng/μL). The mixture was injected into single-cell fertilized eggs of C57BL/6 mice by FemtoJet 5247 microinjection system, and the injected fertilized eggs were transplanted into surrogate female mice. F_0 generation mice were obtained after about 19–21 days of gestation. The ear tissue of 2-week-old mice was collected to obtained genomic DNA, and the following primers were used to identify the genotypes of mice: RNF5-Check F1: 5'-CTGGGGG TACTGAGGGCTAC-3', RNF5-check R1: 5'-GCCCTCT GGTCATCTGAAAA-3'. The selected founder mice were then multiplied and constructed until RNF5-/- mice were obtained for subsequent experiments.

9-11-week-old male C57BL/6 wild type (WT) and RNF5-KO mice weighted 26–28 g were adopted in this study. WT mice used for experiments were purchased from Beijing Vital River Laboratory Animal Technology Co., Ltd. (Beijing, China), and all mice were housed in a

specific pathogen-free animal laboratory of Renmin Hospital of Wuhan University with a temperature (24±2℃) and humidity (40–70%) controlled environment with a 12 h light-dark cycle. Water and food were available *adlibitum* to all mice in experiments. All animal experiments were performed according to the guidelines of the Guide for the Care and Use of Laboratory Animals published by the National Institutes of Health.

Left anterior descending (LAD) coronary artery ligation was performed as described [28, 29]. Briefly, sodium pentobarbital (50 mg/kg, i.p.) was used to anesthetize mice, and the adequacy of anaesthesia was confirmed by the absence of a reflex response to foot squeeze. A left thoracotomy was performed at the third or fourth intercostal space, the pericardium was opened, and the proximal LAD was then encircled under the tip of the left atrial appendage and ligated using a 7–0 silk suture. In sham-operated mice, the LAD was encircled without ligation. All surgeries and subsequent analyses were performed in a blinded fashion.

The experimental groups were WT sham (n=10), RNF5-KO sham (n=10), WT MI (n=10) and RNF5-KO MI (n=10). The animals were randomly grouped, and none of the experimental operators were aware of the treatments. After LAD ligation for 24 h, mice were anesthetized and conducted echocardiographic assessment. Then, the mice were sacrificed by intraperitoneal injection of 1.25% tribromoethanol (0.2 mL per 10 g) and perfused transcardially with saline. Then, the infarcted heart tissues of mice were collected, and the tissue was fixed in 4% paraformaldehyde or frozen in liquid nitrogen for subsequent experiments. All analysis were performed blindly.

Echocardiographic assessment

24 h after LAD ligation, the mice were anesthetized with 1.5-2% isoflurane and then performed ultrasound detection using Small Animal Ultrasound Imaging System (VEVO2100,FUJIFILM VISUALSONICS, Canada). The left ventricular end-systolic diameter (LVESd), left ventricular end-diastolic diameter (LVEDd), left ventricular ejection fraction (EF%) and short axis shortening rate (FS%) were measured at the papillary muscle for three consecutive cycles in M-mode echocardiography mode.

Detection of released AST, LDH, CK

The concentrations of alanine aminotransferase (ALT), aspartate aminotransferase (AST), and creatine kinase (CK) in serum were measured by the Fully Automatic Biochemical Analyzer (3110, Hitachi), according to the manufacturer's instructions.

Histopathological analysis

Histological staining was conducted as previously described [29]. Mice heart tissues were immediately fixed in 10% neutral formalin, dehydrated, embedded in paraffin, cut into 5 μm serial paraffin sections, and stained with CD11b (BM3925, Boster), Ly6g (GB11229, Servicebio) antibody or Terminal deoxynucleotidyl transferase dUTP nick end labeling (TUNEL) staining kit (G1501, Servicebio) according to the instructions for immunofluorescence. The nucleus was stained with DAPI. The antibody of RNF5 (A8351, ABclonal) was adopted to do the immunohistochemical staining. The images were observed and obtained using a light microscope (ECLIPSE 80i, Nikon), and analyzed with Image Pro Plus (Version 6.0) software.

Adenovirus construction

The adenovirus selected short hairpin RNA targeting RNF5 (Adsh*RNF5*) was subcloned into adenovirus to knock down RNF5, and an AdshRNA adenovirus was used as the control. The adenovirus overexpressing RNF5 was purchased from Han Heng Biotechnology Co., LTD, and adenovirus with GFP overexpression served as control. A 150 ~ 200 MOI value (Particle/cell multiplicity of infection) was adopted to decide the adenovirus usage amount infected with cardiomyocytes for 6 h. The primers used are as follows:

Adsh*RNF5*-rat-F: CCGGGCGACCTTCGAATGTAATATACTCGAGTATATTACATTCGAAGGTCG- CTTTTTG.

Adsh*RNF5*-rat-R: AATTCAAAAAGCGACCTTCGAATGTAATATACTCGAGTATATTACAT- TCGAAGGTCGC.

Isolation, culture and oxygen-glucose deprivation(OGD) treatment of primary cardiomyocytes

The hearts of 1-2-day-old SD rats were taken and the blood vessels were removed. The hearts were cut into 1–2 cubic millimeters tissue blocks and digested with 0.125% trypsin to obtain neonatal rat cardiomyocytes (NRCMs). DMEM/F12 (C11330, Gibco) medium containing 10% fetal bovine serum (FBS, 10,099,141 C, GIBCO), 1% penicillin/streptomycin (PS, 15140-122, GIBCO), and 5-bromodeoxyuridine (0.1 mM, B5002- 250MG, sigma) were supplied to culture NRCMs for 24 h. After infected with the corresponding adenovirus, NRCMs were treated with serum-free medium for 12 h, and then stimulated with serum-free, glucose-free and sodium pyruvate-free DMEM (Gibco). The cells were cultured in an incubator containing 95% N_2 and 5% CO_2 for 24 h. The control cells were not subjected to hypoxia with DMEM/F12 medium.

iASK1 treatment: during OGD treatment, the inhibitor of ASK1 activation, GS-4997 (1148428-04-3, Selleck) was added at a concentration of 80 μM. DMSO was used as control.

Cell counting kit 8 (CCK-8) assay

The cell activity of NRCMs was detected by using CCK-8 kit (44,786, Dojindo) according to the manufacturer's guideline. The NRCMs infected with corresponding adenovirus were inoculated into 96-well plates (167008, Thermo Fisher Scientific) and 3 cell-free wells were served as blank controls. And the OGD treatment was performed during 24 h incubation. Then the medium was replaced to CCK8 reaction solution and incubated at 37 ℃ for 2 h. The absorbance value (OD) at 450 nm was measured and the data was recorded.

Quantitative real-time PCR

The TRIzol reagent (15596-026, Invitrogen) was adopted to perform the RNA extraction of the heart tissues or cardiomyocytes under the guidelines of manufacturer. After fragmentated by ultra-sonication in TRIzol reagent, the RNAs were acquired. Transcriptor First Strand cDNA Synthesis Kit (R323-01, Vazyme) was applied to complete the first strand synthesis. The PCR (Polymerase chain reaction) system was composed of SYBR Green PCR Master Mix (Q311-02, Vazyme), the primers and cDNA (Complementary DNA). LightCycler 480 System (Roche) as per the established protocol was adopted to do the quantification and the followed analysis. The primers used in this study were as follows:

Gene names	Sequences (5′-3′)	
RNF5 (Mouse)	Forward	GAATGCCCGGTGTGTAAAGC
	Reverse	GGGGTGGAGTTTTCAATCTGG
TNF-α (Mouse)	Forward	CATCTTCTCAAAATTCGAGTGACAA
	Reverse	TGGGAGTAGACAAGGTACAACCC
IL-6 (Mouse)	Forward	TAGTCCTTCCTACCCCAATTTCC
	Reverse	TTGGTCCTTAGCCACTCCTTC
IL-1β (Mouse)	Forward	CCGTGGACCTTCCAGGATGA
	Reverse	GGGAACGTCACACACCAGCA
CCL2 (Mouse)	Forward	TACAAGAGGATCACCAGCAGC
	Reverse	ACCTTAGGGCAGATGCAGTT
Bax (Mouse)	Forward	TGAGCGAGTGTCTCCGGCGAAT
	Reverse	GCACTTTAGTGCACAGGGCCTTG
Bcl2 (Mouse)	Forward	TGGTGGACAACATCGCCCTGTG
	Reverse	GGTCGCATGCTGGGGCCATATA
GAPDH (Mouse)	Forward	ACTCCACTCACGGCAAATTC
	Reverse	TCTCCATGGTGGTGAAGACA
RNF5 (Rat)	Forward	TATGGTCGAGGGAGCCAGAA
	Reverse	TGAAATCCCCCTGCATCACC
Bax (Rat)	Forward	AGGACGCATCCACCAAGAAG
	Reverse	CAGTTGAAGTTGCCGTCTGC
Bcl2 (Rat)	Forward	CTGGTGGACAACATCGCTCT
	Reverse	GCATGCTGGGGCCATATAGT
GAPDH (Rat)	Forward	CAGTGCCAGCCTCGTCTCAT
	Reverse	AGGGGCATCCACAGTCTTC

Western blotting

RIPA buffer (65 mM Tris-HCl pH 7.5, 150 mM NaCl, 1 mM EDTA, 1% NP-40, 0.5% sodium deoxycholate, 0.1% SDS) with protease inhibitors (04693132001, Roche) facilitated by ultra-sonication was applied to acquire the protein in tissues, while the SDS lysis buffer (50 mM Tris-HCl pH 6.8, 2% SDS, 10% Glycerol) with protease inhibitors was used for protein extraction of cardiomyocytes. BCA Protein Assay Kit (23,225, Thermo Fisher Scientific, USA) was used for the protein quantification, and SDS-PAGE gels as well as PVDF membranes (IPVH00010, Millipore) were used for protein separation and transfer. The blocking was conducted in 5% skim milk for 1 h at room temperature. After the corresponding first antibodies were incubated with the membranes at 4℃ overnight, the corresponding second antibodies (115-035-003 or 111-035-003, Jackson ImmunoResearch Laboratories, USA) were incubated with the membranes at room temperature for 1 h. The ECL Western blotting Substrate kit (BLWB021-100ML, BioLight, China) and the Chemi-DocTM XRS+Imaging System (Bio-Rad, USA) were applied to detect and visualize the proteins. The first antibodies used in this research were as follows:

Antibody	Catalogue number	Manufacturer	Source	Dilution
RNF5	A8351	ABclonal	rabbit	1:1000
p-IKKβ	2697	CST	rabbit	1:1000
IKKβ	A0714	ABclonal	rabbit	1:1000
IKBα	4814	CST	mouse	1:1000
p-p65	3033	CST	rabbit	1:1000
p65	8242	CST	rabbit	1:1000
Bax	A19684	ABclonal	rabbit	1:1000
Bcl2	A19693	ABclonal	rabbit	1:1000
C-Caspase3	9664	CST	rabbit	1:1000
p-ASK1	3765	CST	rabbit	1:1000
ASK1	A12458	ABclonal	rabbit	1:1000
p-JNK	4668	CST	rabbit	1:1000
JNK	9252	CST	rabbit	1:1000
p-p38	4511	CST	rabbit	1:1000
p38	9212	CST	rabbit	1:1000
GAPDH	2118	CST	rabbit	1:5000

Statistical analysis

The data in this research was given as mean±standard deviation (SD). Shapiro Wilk test was used to compare the normal distribution of data. The significant differences between two different groups were assessed by the Student's *t*-test, while One-way or two-way analysis of variance (ANOVA) was performed for data comparison between multiple groups with corrected by the Bonferroni test (equal variances assumed) or Tamhane's T2 test (equal variances not assumed) as the data conforms to the normal distribution. If not, a non-parametric test Mann Whitney test for two groups or Kruskal Wallis test

for multiple groups was conducted. *P* value of less than 0.05 was applied to indicate the significance.

Results

RNF5 was downregulated in infarcted heart tissues of mouse and NRCMs subjected to OGD treatment

To investigate the correlation between RNF5 and MI, we analyzed the mRNA and protein expression levels of RNF5 in different MI models in vivo and in vitro. As shown, the mRNA and protein levels of RNF5 were significantly reduced in hearts of mice suffered MI surgery compared to that in the sham group (Fig. 1A, B). The same results were also observed by immunohistochemical staining (Fig. 1C). Furthermore, in NRCMs subjected to OGD treatment, both the mRNA and protein expression levels of RNF5 were significantly downregulated (Fig. 1D, E). These findings collectively suggest an involvement of RNF5 in the regulation of MI.

Blocking RNF5 exacerbates mouse heart dysfunction and injury after acute MI

To evaluate the impact of RNF5 on acute MI, we generated RNF5-knockout (RNF5-KO) mice and subjected them to LAD surgery. The protein expression of RNF5 was analyzed using Western blotting, confirming the successful establishment of RNF5-KO mice (Fig. 2A).

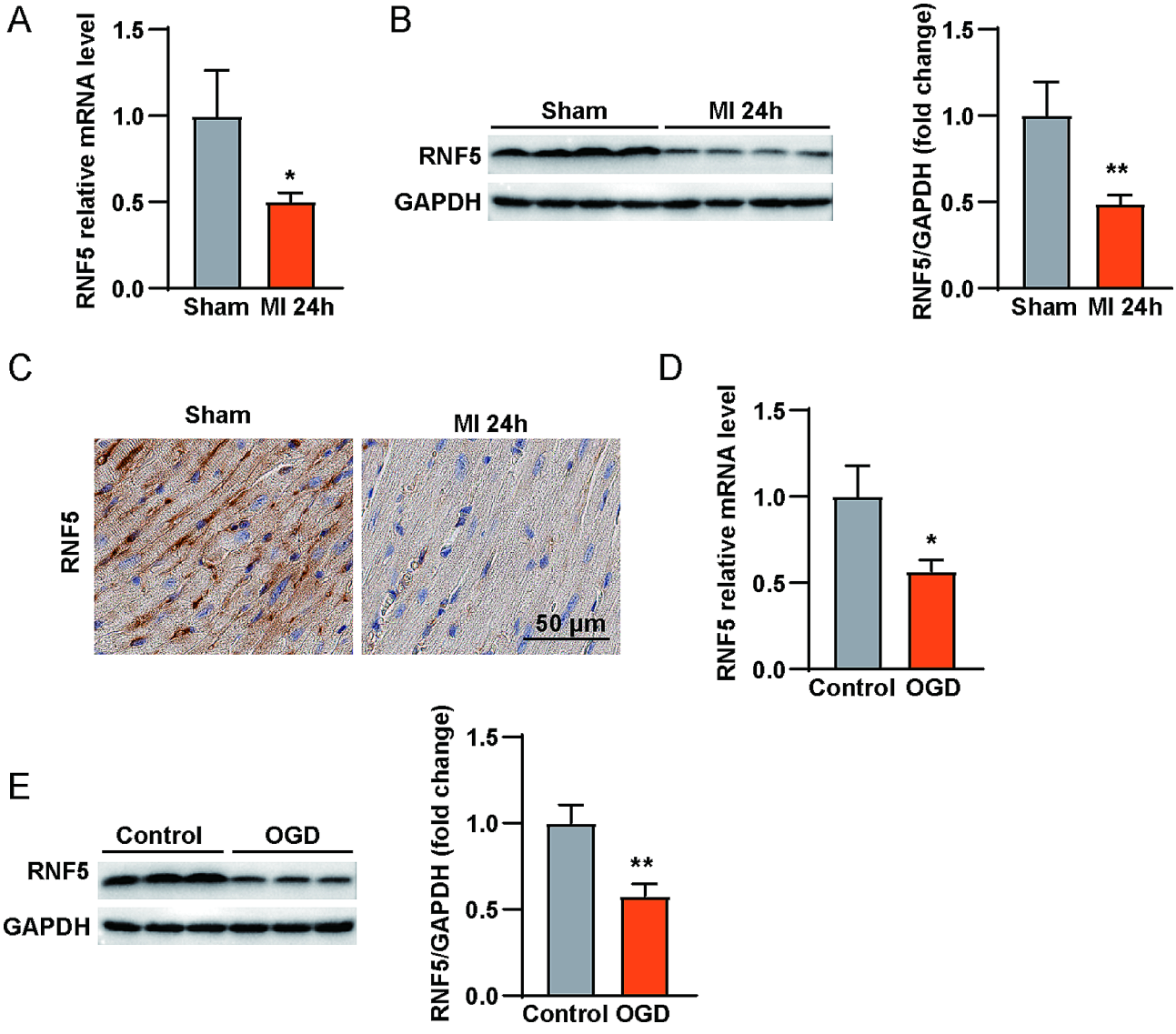

Fig. 1 RNF5 was down-regulated in the hearts of infarcted mice and NRCMs subjected to OGD. (**A**) RT-qPCR results of *RNF5* in the hearts of sham and MI group mice ($n=5$). (**B**) Western blot (Left, $n=4$) and quantification results (Right, $n=5$) of RNF5 in the hearts of sham and MI group mice. (**C**) Representative immunohistochemical staining images of RNF5 expression in the heart samples of sham and MI group mice (Scale bar = 50 μm) ($n=4$). (**D**) RT-qPCR results of *RNF5* in the NRCMs subjected to OGD treatment ($n=3$). (**E**) Western blot (Left) and quantification results (Right) of RNF5 in the NRCMs subjected to OGD treatment ($n=3$). For A, B, D and E, statistical analysis was performed by a two-tailed Student's *t*-test. * $p<0.05$, ** for $p<0.01$.

Following MI or sham surgery, ultrasonic examination was performed before the end of the experiment, and the results showed that the MI surgery resulted in significant increases in LVEDd and LVESd, and significant downregulation of EF% and FS%. Loss of RNF5 promoted the changes of LVEDd and EF% caused by MI surgery, but had no significant effect on LVESd and FS% (Fig. 2B-E). Furthermore, the levels of heart injury-related enzymes, including AST, LDH, and CK were not significantly different between the two sham groups, but were notably increased in MI model group, which indicated that the model was successfully established. Moreover, the enzyme contents in RNF5-KO mice were even more elevated than those in wild-type mice following MI surgery (Fig. 2F-H). These results suggest that RNF5 knockout exacerbated mouse heart injury after acute MI.

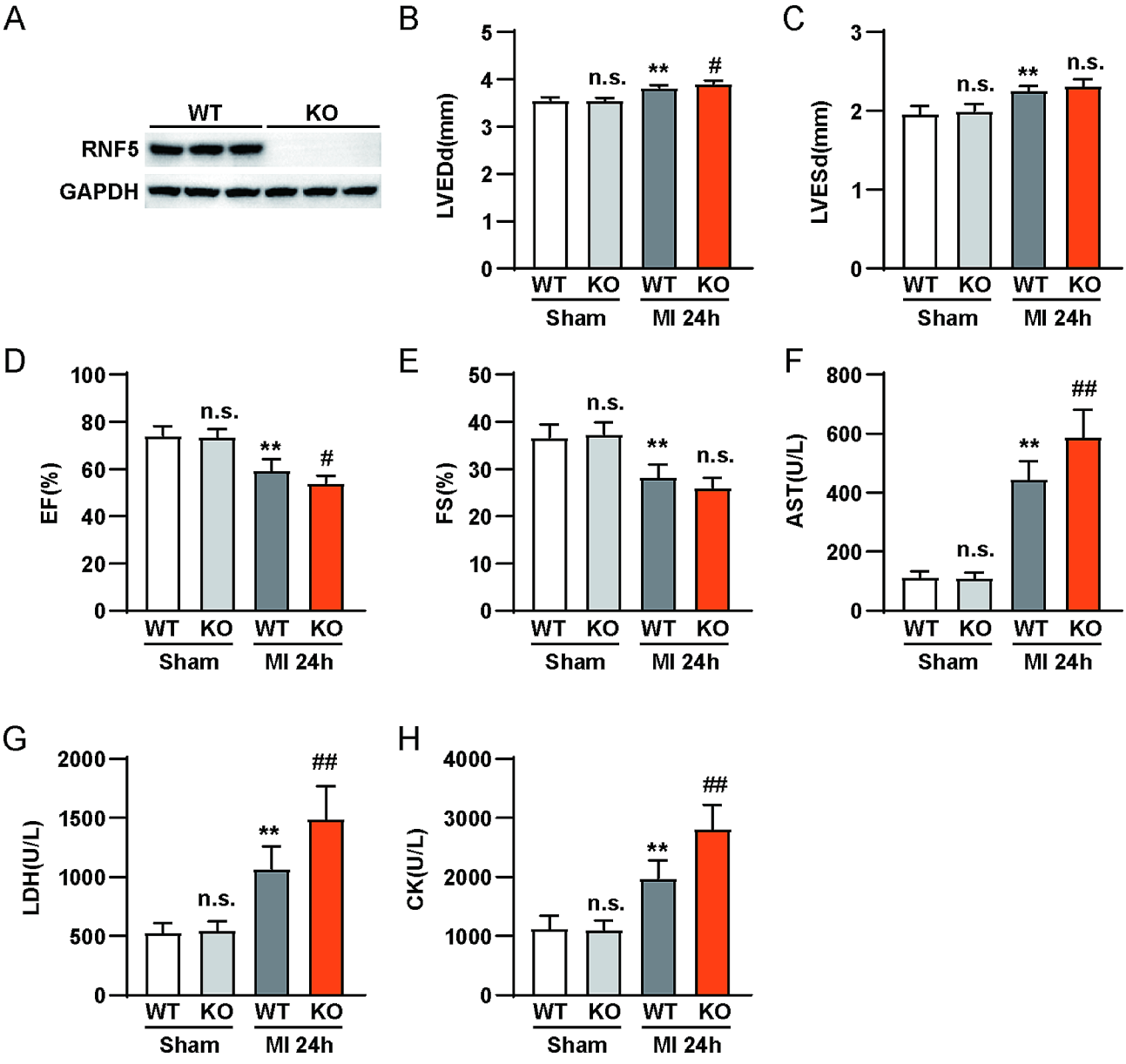

Fig. 2 RNF5 knockout exacerbated heart dysfunction after MI in vivo. (**A**) The Western blot results of RNF5 in the hearts of WT and RNF5-KO mice. $n = 3$ per group. **(B-E)** Echocardiography measurements results including LVEDd **(B)**, LVESd **(C)**, EF% **(D)** and FS% **(E)** of WT and RNF5-KO mice subjected to MI or Sham surgery ($n = 10$ mice per group). (**F-H**) The content variations of representative index enzymes, including AST **(F)**, LDH **(G)** and CK **(H)**, in WT and RNF5-KO mice hearts subjected to or not to MI surgery ($n = 10$). For statistical analysis, One-way ANOVA analysis was used. n.s., no significance, and ** $p < 0.01$ compared with the WT sham group; #, $p < 0.05$, ##, $p < 0.01$ compared with the WT MI group.

RNF5 deficiency increases the inflammatory response and apoptosis in mouse hearts after acute MI

As the inflammatory response and cell apoptosis during acute MI are important events, we wanted to explore whether RNF5 could affect the inflammatory response and cell apoptosis. The infiltration of CD11B and Ly6g positive cells in the heart tissue was analyzed by immunohistochemistry. And the results showed that MI surgery enhanced the integral inflammatory response and RNF5 deficiency promoted infarct-induced inflammatory infiltration of heart tissues (Fig. 3A, B). Consistently, the mRNA expression levels of *Tnf* (*tumor necrosis factor*),

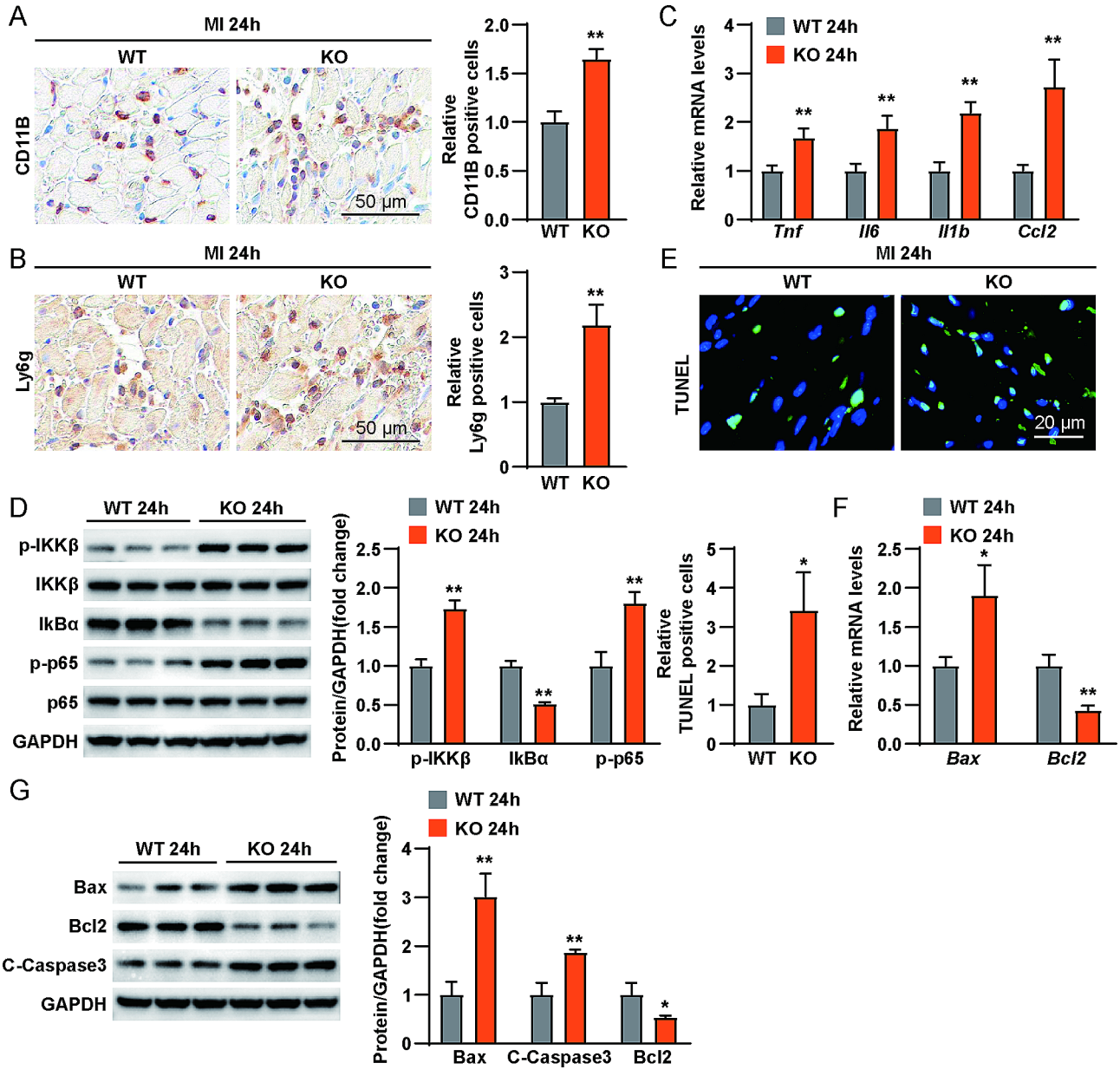

Fig. 3 RNF5 knockout increased inflammatory response and apoptosis after MI in vivo. (**A**) Representative images (Left) and quantitative results (Right) of CD11B immunohistochemical staining of heart sections of the two groups of mice ($n=6$). Scale bar, 50 μm. **(B)** Representative images and quantitative results of Ly6g immunohistochemical staining of heart sections of the two groups of mice ($n=6$). Scale bar, 50 μm. (**C**) RT-PCR results of inflammatory responses associated genes including *Tnf*, *Il6*, *Il1b*, and *Ccl2* in WT and RNF5-KO mice subjected to MI surgery ($n=4$). (**D**) Western blot (Left) and quantification results (Right) of NF-κB signaling pathway-related proteins in wild type and RNF5-KO mice subjected to MI surgery ($n=3$). GAPDH was used as loading control. (**E**) Representative images (Up) and quantitative results (Down) of TUNEL staining of mice heart tissues sections from the indicated group ($n=4$). Scale bar, 20 μm. (**F**) RT-PCR results of apoptosis-related genes in wild type and RNF5-KO mice subjected to MI surgery ($n=4$). The RNA expression levels were normalized to *Gapdh*. (**G**) Western blot (Left) and quantification results (Right) of apoptosis-related proteins in wild type and RNF5-KO mice subjected to MI surgery ($n=3$). GAPDH was used as loading control. For statistical analysis, a two-tailed Student's *t*-test was used. * for $p<0.05$ and ** for $p<0.01$ vs. WT MI 24 h group

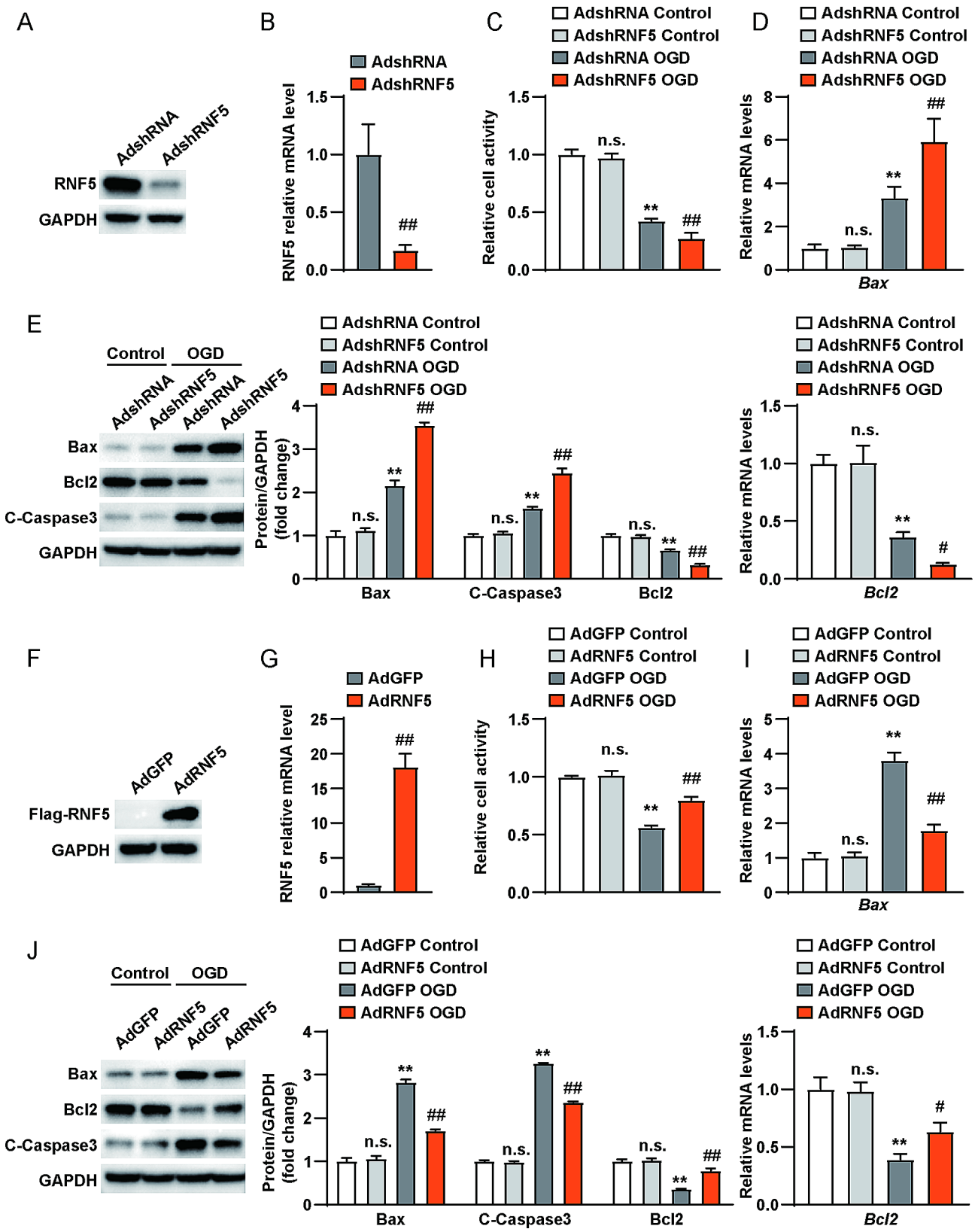

Fig. 4 (See legend on next page.)

(See figure on previous page.)

Fig. 4 RNF5 alleviated cell apoptosis in NRCMs induced by OGD treatment. (**A-B**) Western blot **(A)** and RT-qPCR **(B)** results showed the effectiveness of RNF5 knockdown adenovirus. (**C**) CCK-8 assay showed the cell activity of NRCMs infected with RNF5 knockdown or control adenovirus subjected to or not to OGD treatments. (**D**) RT-PCR results of *Bax* and *Bcl2* genes in NRCMs infected with control or RNF5 knockdown adenovirus subjected to or not to OGD treatments. The RNA expression levels were normalized to *Gapdh*. (**E**) Western blot (Left) and quantification (Right) results of apoptosis-related proteins in NRCMs infected with control or RNF5 knockdown adenovirus subjected to or not to OGD treatments. GAPDH was used as loading control. (**F**, **G**) Western blot **(F)** and RT-PCR **(G)** results showed the effectiveness of RNF5 overexpression adenovirus. (**H**) CCK-8 assay showed the cell activity of NRCMs infected with control or RNF5 overexpression adenovirus subjected to or not to OGD treatments. (**I**) RT-PCR results of *Bax* and *Bcl2* genes in NRCMs infected with control or RNF5 overexpression adenovirus subjected to or not to OGD treatments. The RNA expression levels were normalized to *Gapdh*. (**J**) Western blot (Left) and quantification (Right) results of apoptosis-related proteins in NRCMs infected with control or RNF5 overexpression adenovirus subjected to or not to OGD treatments. $n = 3$ independent repetitions. For B and G, a two-tailed Student's *t*-test was used. For C-E, H-J, One-way ANOVA analysis was used. n.s., no significance, * for $p < 0.05$ and ** for $p < 0.01$ vs. AdshRNA Control group or Ad*GFP* Control group. # for $p < 0.05$ and ## for $p < 0.01$ vs. AdshRNA OGD group or Ad*GFP* OGD group.

interleukin-6 (*Il6*), *Il1b*, and chemokines *CCL2* (*C-C motif chemokine 2*) (Fig. 3C) as well as the protein levels of NF-κB (nuclear factor kappa-B) signaling pathway components, including phosphorylated IKKβ (inhibitor of nuclear factor kappa-B kinase subunit beta, p-IKKβ) and phosphorylated p65 (p-p65) (Fig. 3D) were significantly increased. TUNEL assays showed that RNF5-KO mice showed more serious apoptosis under MI treatments than those in the WT group (Fig. 3E). Correspondingly, the pro-apoptosis molecules including Bax, cleaved Caspase 3 (C-Caspase3) were upregulated, while the anti-apoptosis factor Bcl2 was downregulated in RNF5-KO MI group compared with WT MI group (Fig. 3F, G). Combining these findings, it is concluded that loss of RNF5 exacerbated the inflammatory response and apoptosis in mouse hearts after acute MI surgery.

RNF5 alleviated apoptosis in NRCMs under OGD treatment in vitro

To explore the effects of RNF5 on cardiomyocytes, the NRCMs were separated and subjected to OGD treatment to imitate MI in vitro. The efficacy of RNF5 knockdown adenovirus was analyzed by Western blot and RT-qPCR, and the results showed that the protein and mRNA expression levels of RNF5 were both significantly decreased (Fig. 4A, B). The CCK-8 assay demonstrated that knockdown of RNF5 aggravated OGD-induced cardiomyocyte injury (Fig. 4C). Consistent with the in vivo results, RNF5 knockdown promoted the expression of pro-apoptotic molecules (Bax and C-Caspase 3) induced by ODG and inhibited the expression of anti-apoptotic Bcl2 (Fig. 4D, E). Conversely, Ad*RNF5* adenovirus was used to upregulate the expression of RNF5 in NRCMs (Fig. 4F, G). In contrast to RNF5 knockdown, RNF5 overexpression protected cardiomyocytes from cell injury and apoptosis induced by OGD stimulation (Fig. 4H-J). Together, RNF5 protects against cardiomyocyte apoptosis under OGD treatment.

RNF5 suppresses the ASK1-JNK/p38 signaling pathway in MI

A previous report indicated that RNF5 could regulate hepatic ischemia–reperfusion injury by targeting apoptosis signal-regulating kinase 1 (ASK1) [8]. ASK1 is a key modulator of the ROS-induced extrinsic apoptosis pathway, and ASK1-deficient mice demonstrate that the ROS/ASK1 pathway is involved in necrotic as well as apoptotic cell death, indicating that ASK1 may be a therapeutic target to reduce left ventricular remodeling after MI [30, 31]. To explore the underlying mechanism of RNF5 during MI, we detected the expression levels of phosphorylated ASK1 and ASK1 proteins as well as the downstream signaling molecules including total and phosphorylated JNK, p38 in MI models. We found that RNF5 deficiency or knockdown promoted the phosphorylation of ASK1, JNK and p38 but without affecting the corresponding total proteins (Fig. 5A, B). In contrast, overexpression of RNF5 decreased the protein levels of p-ASK1, p-JNK and p-p38 in NRCMs subjected to OGD treatment (Fig. 5C). Taken together, RNF5 suppresses the ASK1-JNK/p38 signaling pathway in response to MI.

Inhibiting ASK1 activation reverses apoptosis in RNF5-knockdown cardiomyocytes

To analyze whether activated ASK1 mediated RNF5 function during MI, an inhibitor of ASK1 activation (iASK1), GS-4997, was applied to RNF5-knockdown NRCMs. The protein level analysis in the cascade showed that the increase in p-ASK1, p-JNK and p-p38 resulting from RNF5-knockdown was abolished when iASK1 was applied (Fig. 6A). Furthermore, the promotion of cell injury and apoptosis due to RNF5 knockdown was also abolished by iASK1 (Fig. 6B-D). These results suggested that the regulation effect of RNF5 on the apoptosis of cardiomyocytes was mediated by inhibiting the activation of ASK1.

Discussion

Cardiovascular disease, including myocardial infarction (MI), is the leading cause of death globally, with a resurgence in high-income countries and an ongoing rapid

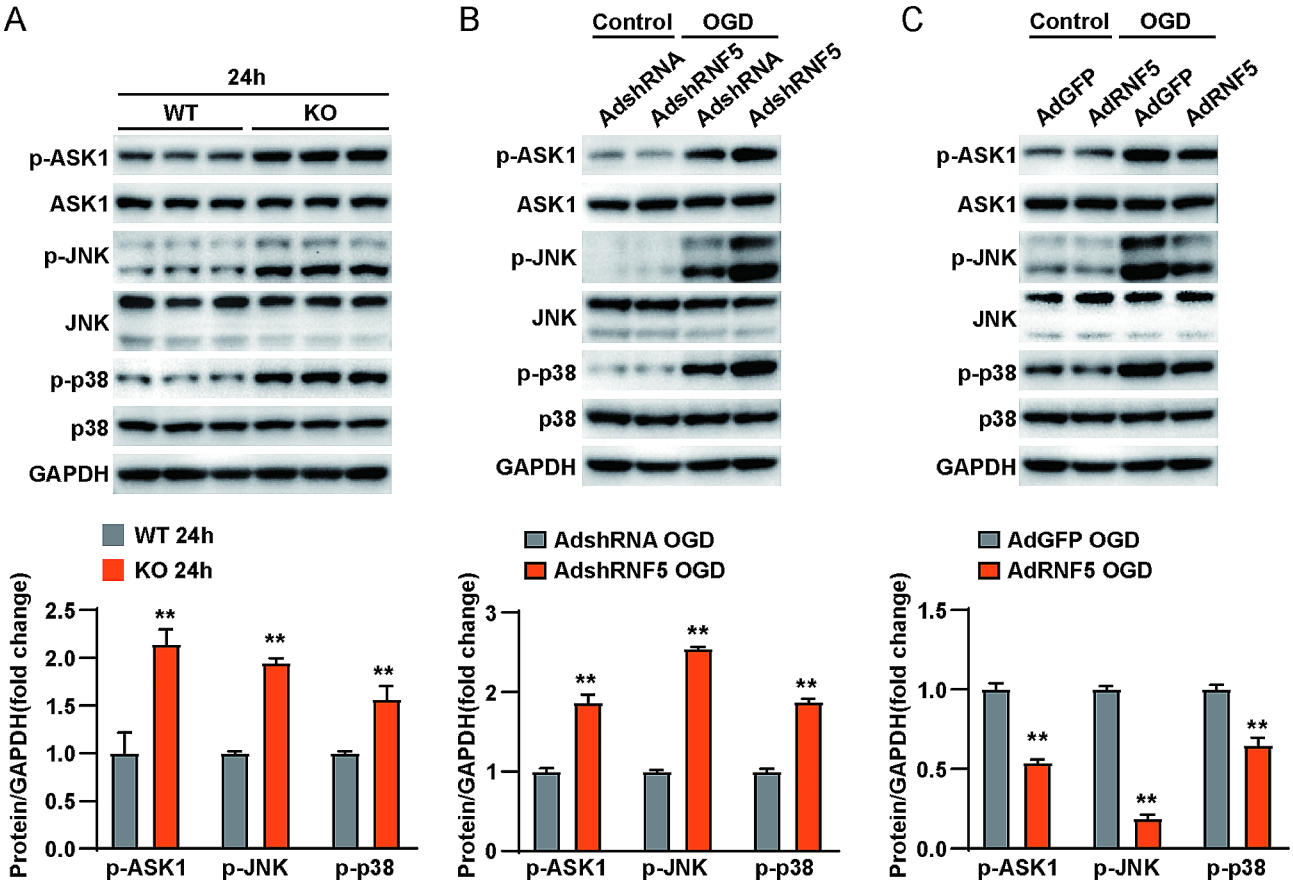

Fig. 5 RNF5 regulated the activation of ASK1-JNK/p38 signaling pathway during MI. (**A**) Western blot (Up) and quantification (Down) results of total and phosphorylated ASK1, JNK and p38 in wild type and RNF5-KO mice heart tissues subjected to MI surgery ($n=3$). (**B**) Western blot (Up) and quantification (Down) results of total and phosphorylated ASK1, JNK and p38 in NRCMs infected with control or RNF5 knockdown adenovirus subjected to or not to OGD treatments. $n=3$ independent repetitions. (**C**) Western blot (Up) and quantification (Down) results of total and phosphorylated ASK1, JNK and p38 in NRCMs infected with control or RNF5 overexpression adenovirus subjected to or not to OGD treatments. $n=3$ independent repetitions. For statistical analysis, a two-tailed Student's *t*-test was used. * for $p<0.05$ and ** for $p<0.01$ vs. WT MI 24 h group or AdshRNA OGD group or Ad*GFP* OGD group

rise in low- and middle-income countries [32]. After MI, myocardial cells undergo significant changes such as inflammation and increased apoptosis, resulting in irreversible damage to myocardial cells [4, 6]. Substantial gaps between pharmacotherapy armament and rising patients highlight the urgency to exploit potent molecular targets. In this study, we discovered that a new component, RNF5, is involved in MI and plays protective roles depending on inhibiting activated ASK1, which may facilitate the development of new therapeutic strategy for MI.

RNF5 is an ER-located ubiquitin E3 ligase and has been previously investigated in tumor progression, innate immune response, and especially cystic fibrosis therapy development, mainly through ubiquitination-mediated protein degradation [8, 12–14]. However, only a few studies have focused on cardiovascular disease. In pathological cardiac hypertrophy, RNF5 deficiency aggravated TAC-induced cardiac remodeling, myocardial fibrosis, and inflammation [25]. In NASH, RNF5 knockout significantly exacerbated hepatic steatosis, the inflammatory response and fibrosis in mice with diet-induced NASH mice [26]. Moreover, in OGD-induced rat H9C2 cell lines, RNF5 overexpression reversed the OGD/R-induced decreases in cell viability, the apoptosis rate and inflammatory factor release [27]. Our findings represent a novel connection between RNF5 and myocardial infarction, thereby broadening the understanding of RNF5's function. We found that the deficiency of RNF5 promoted the changes of LVEDd and EF% caused by LAD surgery, but had no significant effect on LVESd and FS%. This may be due to the fact that our trial was set for a short period of time after LAD surgery, and extending the trial time may lead to an enhanced effect of RNF5 on cardiac dysfunction, which requires further study. In addition, RNF5 knockout aggravated the inflammatory responses and subsequent apoptosis after MI, which was consistent with previously found functions in cardiovascular-related diseases and implied that improving RNF5

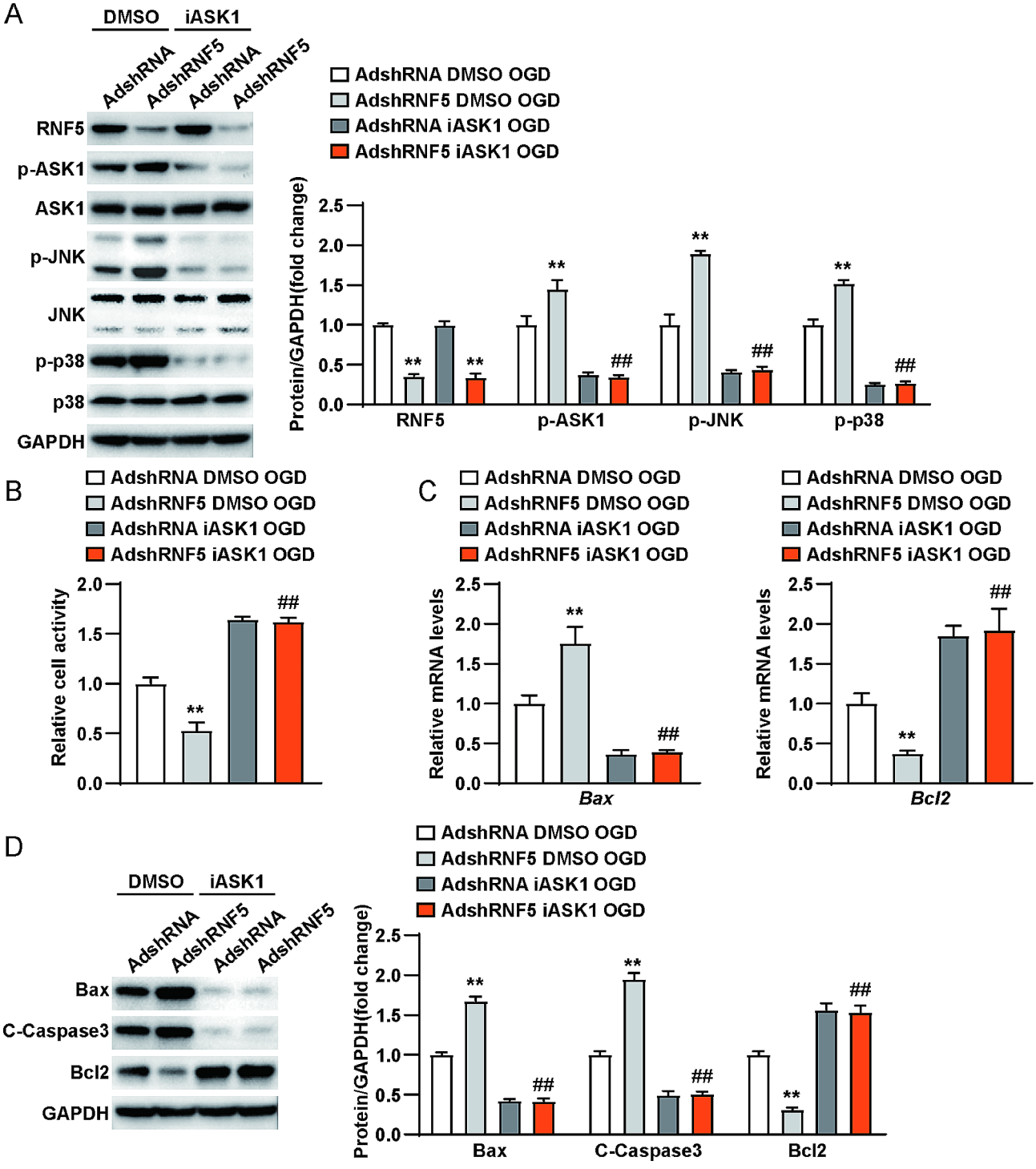

Fig. 6 Treatment of iASK1 inhibited the promoting effect of RNF5 knockdown on OGD-induced apoptosis of NRCMs. (**A**) Western blot (Left) and quantification (Right) results of RNF5, total and phosphorylated ASK1, JNK and p38 in NRCMs harboring control or RNF5 knockdown adenovirus subjected to OGD treatments with or without iASK1 addition. (**B**) CCK-8 assay showed the cell activity in in NRCMs harboring control or RNF5 knockdown adenovirus subjected to OGD treatments with or without iASK1 addition. (**C**) RT-qPCR results of *Bax* and *Bcl2* in NRCMs infected with control or RNF5 knockdown adenovirus subjected to OGD treatments with or without iASK1 addition. (**D**) Western blot (Left) and quantification (Right) results of apoptosis-related proteins in NRCMs harboring control or RNF5 knockdown adenovirus subjected to OGD treatments with or without iASK1 addition. $n = 3$ independent repetitions. For statistical analysis, One-way ANOVA analysis was used. * for $p < 0.05$ and ** for $p < 0.01$ vs. AdshRNA DMSO OGD group. # for $p < 0.05$ and ## for $p < 0.01$ vs. Adsh*RNF5* DMSO OGD group.

content might be a feasible alternative for therapeutic development.

A small drug-like compound Analog-1, which has been defined as an activator of RNF5, could enhance the activity of RNF5 but does not affect its protein expression [22, 33]. It has been found that Analog-1 significantly reduced the viability of SH-SY5Y and MZ2-MEL cells, but was totally ineffective in normal human fibroblasts. This proves that in different types of cells, Analog-1 has different functions. In addition, Analog-1 has been shown to promote oxidative stress-induced apoptosis [34]. Since there are no reports on the function of Analog-1 in myocardial infarction, it is uncertain whether Analog-1 can play a protective role in myocardial infarction by activating RNF5.

Previous reports have primarily focused on RNF5 functioning as a ubiquitin ligase to regulate protein stability through ubiquitination-mediated protein degradation. The most investigated substrates of RNF5 include STING, MAVS, and CFTR [13, 14, 21]. In antiviral responses, RNF5 interacts with STING through its transmembrane domain and targets MITA at Lys150 for ubiquitination and degradation after viral infection [13]. In another study, the intermediate domain plus either the RING or the transmembrane domain of RNF5 was sufficient for its interaction with MAVS, and RNF5 targeted MAVS at K362 and K461 for ubiquitination and degradation after viral infection [21]. In cystic fibrosis, the most common mutation in the gene encoding the CF transmembrane conductance regulator (CFTR), the deletion of phenylalanine 508 (F508del), is associated with misfolding and premature degradation of the mutant protein, impairing CFTR trafficking [14, 23]. RNF5 could promote F508del-CFTR degradation at early stages of CFTR biosynthesis and its inhibition resulted in the rescue of F508del-CFTR phenotypes [14, 24]. Comparatively, in our research, we discovered that RNF5 played protective roles after MI by inhibiting ASK1 phosphorylation, which seemed to be an atypical function of RNF5. Whether RNF5 changes the phosphorylation of ASK1 directly through its E3 ligase function or indirectly recruits another component, such as phosphatases, still needs more investigation.

Conclusion

Our investigation found that RNF5 was significantly downregulated in infarcted mice hearts. RNF5 knockout exacerbated MI surgery-induced heart dysfunction, inflammatory responses and apoptosis in infarcted mouse hearts. Consistently, RNF5 knockdown decreased the cell activity of NRCMs and promoted cell apoptosis after OGD treatment, while RNF5 overexpression resulted in the opposite results. These results first prove that RNF5 plays a protective role in MI. Furthermore, the kinase cascade initiated by phosphorylated ASK1 was negatively regulated by RNF5, and the inhibition of activated ASK1 abolished RNF5 knockdown-mediated promoting effects on OGD surgery-induced apoptosis in NRCMs. These findings revealed a new component of RNF5 functioning in MI, and RNF5-ASK1 signaling might indicate the possibility of new therapeutic strategy development for MI.

Supplementary Information

The online version contains supplementary material available at https://doi.org/10.1186/s12872-024-04070-z.

Supplementary Material 1

Supplementary Material 2

Supplementary Material 3

Author contributions

C.W., G.W., H.W. and J.Z. participated in the research design, the analysis of the results and the writing of the paper. H.W. and J.Z. performed the cell experiments in this investigation. J.Z. and Z.L. were in charge of molecular biological associated detection. B.D. and Z.T. performed the animal experiments. All authors have read and agreed to the published version of the manuscript.

Funding

Not applicable.

Data availability

No datasets were generated or analysed during the current study.

Declarations

Ethics approval and consent to participate

All animal use protocols were approved by the Animal Care and Use Committee of Renmin Hospital of Wuhan University (20230405 C). This study is reported in accordance with ARRIVE guidelines (https://arriveguidelines.org).

Consent for publication

Not applicable.

Competing interests

The authors declare no competing interests.

Received: 14 May 2024 / Accepted: 22 July 2024
Published online: 05 August 2024

References

1. Thygesen K, Alpert JS, Jaffe AS, Chaitman BR, Bax JJ, Morrow DA, White HD. Fourth universal definition of myocardial infarction (2018). J Am Coll Cardiol. 2018;72(18):2231–64.
2. Virani SS, Alonso A, Benjamin EJ, Bittencourt MS, Callaway CW, Carson AP, Chamberlain AM, Chang AR, Cheng S, Delling FN, et al. Heart disease and stroke statistics—2020 update: a report from the American Heart Association. Circulation. 2020;141(9):e139–596.
3. Samsky MD, Morrow DA, Proudfoot AG, Hochman JS, Thiele H, Rao SV. Cardiogenic shock after Acute Myocardial Infarction A Review. Jama-J Am Med Assoc. 2021;326(18):1840–50.
4. Yap J, Irei J, Lozano-Gerona J, Vanapruks S, Bishop T, Boisvert WA. Macrophages in cardiac remodelling after myocardial infarction. Nat Reviews Cardiol. 2023;20(6):373–85.
5. Kologrivova I, Shtatolkina M, Suslova T, Ryabov V. Cells of the Immune System in Cardiac Remodeling: main players in resolution of inflammation and repair after myocardial infarction. Front Immunol. 2021;12.

6. Lin X, Liu W, Chu Y, Zhang H, Zeng L, Lin Y, Kang K, Peng F, Lin J, Huang C et al. Activation of AHR by ITE improves cardiac remodelling and function in rats after myocardial infarction. ESC Heart Fail. 2023.
7. Farokhian A, Rajabi A, Sheida A, Abdoli A, Rafiei M, Jazi ZH, Asouri SA, Morshedi MA, Hamblin MR, Adib-Hajbagheri P, et al. Apoptosis and myocardial infarction: role of ncRNAs and exosomal ncRNAs. Epigenomics. 2023;15(5):307–34.
8. Matsuda N, Suzuki T, Tanaka K, Nakano A. RMA1, a novel type of RING finger protein conserved from *Arabidopsis* to human, is a membrane-bound ubiquitin ligase. J Cell Sci. 2001;114(Pt 10):1949–57.
9. Ding M, Fang H, Zhang J, Shi J, Yu X, Wen P, Wang Z, Cao S, Zhang Y, Shi X, et al. E3 ubiquitin ligase RING finger protein 5 protects against hepatic ischemia reperfusion injury by mediating phosphoglycerate mutase family member 5 ubiquitination. Hepatology. 2022;76(1):94–111.
10. Huang EY, To M, Tran E, Dionisio LTA, Cho HJ, Baney KLM, Pataki CI, Olzmann JA, Sommer T. A VCP inhibitor substrate trapping approach (VISTA) enables proteomic profiling of endogenous ERAD substrates. Mol Biol Cell. 2018;29(9):1021–30.
11. Tcherpakov M, Delaunay A, Toth J, Kadoya T, Petroski MD, Ronai ZA. Regulation of endoplasmic reticulum-associated degradation by RNF5-dependent ubiquitination of JNK-associated membrane protein (JAMP). J Biol Chem. 2009;284(18):12099–109.
12. Jeon YJ, Khelifa S, Ratnikov B, Scott DA, Feng Y, Parisi F, Ruller C, Lau E, Kim H, Brill Laurence M, et al. Regulation of glutamine carrier proteins by RNF5 determines breast cancer response to ER stress-inducing chemotherapies. Cancer Cell. 2015;27(3):354–69.
13. Zhong B, Zhang L, Lei C, Li Y, Mao A, Yang Y, Wang Y, Zhang X, Shu H. The ubiquitin ligase RNF5 regulates antiviral responses by mediating degradation of the adaptor protein MITA. Immunity. 2009;30(3):397–407.
14. Tomati V, Sondo E, Armirotti A, Caci E, Pesce E, Marini M, Gianotti A, Ju Jeon Y, Cilli M, Pistorio A, et al. Genetic inhibition of the ubiquitin ligase RNF5 attenuates phenotypes associated to F508del cystic fibrosis mutation. Sci Rep. 2015;5(1):12138.
15. Karijolich J, Li X, Wang F, Zhang X, Sun Q, Kuang E. Suppression of KSHV lytic replication and primary effusion lymphoma by selective RNF5 inhibition. PLoS Pathog. 2023;19(1):e1011103.
16. Khateb A, Deshpande A, Feng Y, Finlay D, Lee JS, Lazar I, Fabre B, Li Y, Fujita Y, Zhang T, et al. The ubiquitin ligase RNF5 determines acute myeloid leukemia growth and susceptibility to histone deacetylase inhibitors. Nat Commun. 2021;12(1):5397.
17. Zhang Y, Li J, Chen H, Zhang C, You S, Zhao Y, Lin X, Yu Y, Fang F, Fang T, et al. RING-finger protein 5 promotes hepatocellular carcinoma progression and predicts poor prognosis. Hum Cell. 2021;34(2):530–8.
18. Li Y, Tinoco R, Elmén L, Segota I, Xian Y, Fujita Y, Sahu A, Zarecki R, Marie K, Feng Y, et al. Gut microbiota dependent anti-tumor immunity restricts melanoma growth in Rnf5–/– mice. Nat Commun. 2019;10(1):1492.
19. Li X, Wang F, Huang L, Yang M, Kuang E. Downregulation of EphA2 stability by RNF5 limits its tumor-suppressive function in HER2-negative breast cancers. Cell Death Dis. 2023;14(10):662.
20. Lowen AC, Zeng Y, Xu S, Wei Y, Zhang X, Wang Q, Jia Y, Wang W, Han L, Chen Z, et al. The PB1 protein of influenza a virus inhibits the innate immune response by targeting MAVS for NBR1-mediated selective autophagic degradation. PLoS Pathog. 2021;17(2):e1009300.
21. Zhong B, Zhang Y, Tan B, Liu T, Wang Y, Shu H. The E3 ubiquitin ligase RNF5 targets virus-induced signaling adaptor for ubiquitination and degradation. J Immunol. 2010;184(11):6249–55.
22. Li ZL, Hao PF, Zhao ZL, Gao WY, Huan C, Li LT, Chen X, Wang H, Jin NY, Luo ZQ et al. The E3 ligase RNF5 restricts SARS-CoV-2 replication by targeting its envelope protein for degradation. Signal Transduct Tar. 2023;8(1).
23. Sondo E, Falchi F, Caci E, Ferrera L, Giacomini E, Pesce E, Tomati V, Mandrup Bertozzi S, Goldoni L, Armirotti A, et al. Pharmacological inhibition of the ubiquitin ligase RNF5 rescues F508del-CFTR in cystic fibrosis airway epithelia. Cell Chem Biology. 2018;25(7):891–e905898.
24. Brusa I, Sondo E, Pesce E, Tomati V, Gioia D, Falchi F, Balboni B, Ortega Martínez JA, Veronesi M, Romeo E, et al. Innovative strategy toward mutant CFTR rescue in cystic fibrosis: design and synthesis of thiadiazole inhibitors of the E3 ligase RNF5. J Med Chem. 2023;66(14):9797–822.
25. Song S, Shi C, Bian Y, Yang Z, Mu L, Wu H, Duan H, Shi Y. Sestrin2 remedies podocyte injury via orchestrating TSP-1/TGF-beta1/Smad3 axis in diabetic kidney disease. Cell Death Dis. 2022;13(7):663.
26. Yang Q, Chen X, Zhang Y, Hu S, Hu F, Huang Y, Ma T, Hu H, Tian H, Tian S, et al. The E3 ubiquitin ligase RING finger protein 5 ameliorates NASH through ubiquitin-mediated degradation of 3-hydroxy-3-methylglutaryl CoA reductase degradation protein 1. Hepatology. 2021;74(6):3018–36.
27. Wu Y, Chen X, Bao Y. Ring-finger protein 5 attenuates oxygen-glucose deprivation and reperfusion-induced mitochondrial dysfunction and inflammation in cardiomyocytes by inhibiting the S100A8/MYD88/NF-κB axis. Chin J Physiol. 2023;66(4):228–38.
28. Wan N, Liu X, Zhang X, Zhao Y, Hu G, Wan F, Zhang R, Zhu X, Xia H, Li H. Toll-interacting protein contributes to mortality following myocardial infarction through promoting inflammation and apoptosis. Br J Pharmacol. 2015;172(13):3383–96.
29. Bao M, Cai Z, Zhang X, Li L, Liu X, Wan N, Hu G, Wan F, Zhang R, Zhu X et al. Dickkopf-3 protects against cardiac dysfunction and ventricular remodelling following myocardial infarction. Basic Res Cardiol. 2015;110(3).
30. Hori M, Nishida K. Oxidative stress and left ventricular remodelling after myocardial infarction. Cardiovascular Res. 2008;81(3):457–64.
31. Lai J, Li A, Yue L, Zhong H, Xu S, Liu X. Participation of ASK-1 in the cardiomyocyte-protective role of mechanical ventilation in a rat model of myocardial infarction. Experimental Biology Med (Maywood). 2023;3:15353702231191205.
32. Figtree GA, Broadfoot K, Casadei B, Califf R, Crea F, Drummond GR, Freedman JE, Guzik TJ, Harrison D, Hausenloy DJ, et al. A call to action for new global approaches to cardiovascular disease drug solutions. Circulation. 2021;144(2):159–69.
33. Sondo E, Falchi F, Caci E, Ferrera L, Giacomini E, Pesce E, Tomati V, Bertozzi SM, Goldoni L, Armirotti A, et al. Pharmacological inhibition of the Ubiquitin Ligase RNF5 rescues F508del-CFTR in cystic fibrosis Airway Epithelia. Cell Chem Biol. 2018;25(7):891–905.
34. Principi E, Sondo E, Bianchi G, Ravera S, Morini M, Tomati V, Pastorino C, Zara F, Bruno C, Eva A et al. Targeting of Ubiquitin E3 ligase RNF5 as a Novel Therapeutic Strategy in Neuroectodermal Tumors. Cancers. 2022;14(7).

Publisher's Note